Bound States of Skyrmions and Merons near the Lifshitz Point

Kharkov, Y. A.; Sushkov, O. P.; Mostovoy, Maxim

[Link to publication in University of Groningen/UMCG research database](#)

Bound States of Skyrmions and Merons near the Lifshitz Point

Y. A. Kharkov,[1] O. P. Sushkov,[1] and M. Mostovoy[2]

[1]*School of Physics, University of New South Wales, Sydney 2052, Australia*
[2]*Zernike Institute for Advanced Materials, University of Groningen, 9747 AG Groningen, Netherlands*

We study topological defects in anisotropic ferromagnets with competing interactions near the Lifshitz point. We show that Skyrmions and bimerons are stable in a large part of the phase diagram. We calculate Skyrmion-Skyrmion and meron-meron interactions and show that Skyrmions attract each other and form ring-shaped bound states in a zero magnetic field. At the Lifshitz point merons carrying a fractional topological charge become deconfined. These results imply that unusual topological excitations may exist in weakly frustrated magnets with conventional crystal lattices.

Introduction.—Some 50 years ago Tony Skyrme identified topologically stable "hedgehoglike" configurations of the meson field with baryons, such as proton and neutron [1]. The ensuing theoretical work showed that Skyrmions indeed provide a semiquantitative description of physical properties of baryons and their interactions [2]. Multi-Skyrmion bound states describe ground states and low-energy excitations of atomic nuclei [3]. Periodic crystals of Skyrmions and half-Skyrmions were used to model nuclear matter [4–6].

Two-dimensional analogs of Skyrme's Skyrmions are relevant topological excitations in many condensed matter systems [7], such as quantum Hall magnets [8,9], spinor Bose-Einstein condensates [10], superfluid ^{3}He [11], chiral liquid crystals [12], and chiral magnets [13], which provide the playground for experimental studies of Skyrmions. Skyrmion crystals and isolated Skyrmions in chiral magnets can be observed by neutron scattering and Lorentz microscopy [14,15], and controlled by ultralow electric currents [16,17], applied electric fields [18,19], and thermal gradients [20], which opened a new active field of research on Skyrmion-based magnetic memories [21–26]. Half-Skyrmions (or merons) carying half-integer topological charge were also discussed theoretically in the context of quantum Hall systems [27], bilayer graphene [28], and chiral magnets [29,30], but so far they eluded experimental detection.

Here, we are interested in magnetic multi-Skyrmion and multimeron configurations with a large topological charge, Q. An example is the Skyrmion crystal in chiral magnets. However, Skyrmions in the crystal can hardly be considered as independent particlelike objects, since to a good approximation this state is a superposition of three spin spirals plus a uniform magnetization [14]. Isolated Skyrmions appear under an applied magnetic field that suppresses modulated spiral and Skyrmion crystal phases and induces a collinear ferromagnetic (FM) state. Skyrmions in chiral magnets repel each other [31], so that multi-Skyrmion states are merely a gas of elementary Skyrmions with $Q = \pm 1$.

It was recently suggested that Skyrmion crystals and isolated Skyrmions can also exist in frustrated magnets with conventional centrosymmetric lattices, where they are stabilized by competing ferromagnetic and antiferromagnetic (AFM) exchange interactions [32–34]. In frustrated magnets, the Skyrmion-Skyrmion interaction potential changes sign as a function of the distance between Skyrmions, which makes possible formation of Skyrmion clusters as well as rotationally symmetric Skyrmions with the topological charge $Q = \pm 2$ [33].

We note that topological excitations in frustrated magnets can be stable even in zero magnetic field. Consider a magnet in which the degree of frustration described by the parameter f that can be varied, e.g., by an applied pressure or a chemical substitution. The phase diagram of such magnets often contains the so-called Lifshitz point (LP), $f = f_*$, which separates the uniform FM state ($f < f_*$) from periodically modulated phases ($f > f_*$). The behavior close to the LP was recently discussed in the context of Bose condensation of multimagnon bound states in quantum low-dimensional systems [35]. Skyrmions, which can be considered as bound states of a large number of magnons, so far were studied in the strongly frustrated regime ($f > f_*$). In this Letter, we focus on the "underfrustrated" side of the LP and show that Skyrmions are stable in a large interval of $f < f_*$. We show that elementary Skyrmions attract each other and can form bound states with an arbitrarily large Q. Surprisingly, despite the attraction, Skyrmions do not aggregate into clusters. Instead, they form topological ring-shaped domain walls.

The aforementioned unusual multi-Q states appear in easy-axis magnets. An easy-plane anisotropy forces Skyrmion to transform into a bound pair of merons with opposite vorticities, each carrying topological charge $Q = \frac{1}{2}$. The lowest-energy multimeron configuration is a square lattice of merons with alternating vorticities. Our results show that stability of Skyrmions and merons does not require strong magnetic frustration, implying that these exotic topological excitations with interesting physical properties can exist in already known magnetic materials. In addition, we find a number of striking similarities

between multi-Q Skyrmions in condensed matter and
nuclear physics.

The model.—We consider classical spins on a square
lattice with competing exchange interactions and magnetic
anisotropy. The energy of the model is

$$E = -J_1 \sum_{\langle i,j \rangle} \mathbf{S}_i \cdot \mathbf{S}_j + J_2 \sum_{\langle\langle i,j \rangle\rangle} \mathbf{S}_i \cdot \mathbf{S}_j + J_3 \sum_{\langle\langle\langle i,j \rangle\rangle\rangle} \mathbf{S}_i \cdot \mathbf{S}_j$$
$$+ \frac{K}{2} \sum_i (1 - (S_i^z)^2), \qquad (1)$$

where $\mathbf{S}_i$ is the spin of unit length at the lattice site i and the
first, second, and third terms describe, respectively, FM
nearest-neighbor and AFM second- and third-neighbor
exchange interactions ($J_1, J_2, J_3 > 0$). The z axis is normal
to the lattice plane (the xy plane) and K is the strength of the
single-ion magnetic anisotropy of easy axis ($K > 0$) or easy
plane ($K < 0$) type. In what follows, energy is measured in
units of $J_1 = 1$ and distances are measured in units of the
lattice constant.

For slowly varying spin textures, Eq. (1) is equivalent to
the continuum model (see e.g., Ref. [36]),

$$E = \frac{1}{2} \int d^2 r \{ \rho(\partial_i \mathbf{S})^2 + b_1[(\partial_x^2 \mathbf{S})^2 + (\partial_y^2 \mathbf{S})^2]$$
$$+ b_2 \partial_x^2 \mathbf{S} \cdot \partial_y^2 \mathbf{S} + K(1 - S_z^2) \}, \qquad (2)$$

where $\rho = J_1 - 2J_2 - 4J_3$, $b_1 = (1/12)(-J_1 + 2J_2 + 16J_3)$,
$b_2 = J_2$ and $i = x, y$. The first term in Eq. (2) is the
$O(3)$ nonlinear sigma model of an isotropic two-
dimensional ferromagnet. The spin stiffness ρ plays the
role of $f_* - f$: in the FM state $\rho > 0$, at the Lifshitz point ρ
vanishes, and for $\rho < 0$, the system has either a spiral or a
columnar antiferromagnetic (CAF) ground state [37], as
shown in Fig. 1(a) [38]. The fourth-order terms in gradients
of $\mathbf{S}$ stabilize the spiral state and determine its wave vector
provided that $b_1 > 0$ and $b_1 + b_2/2 > 0$. These terms also
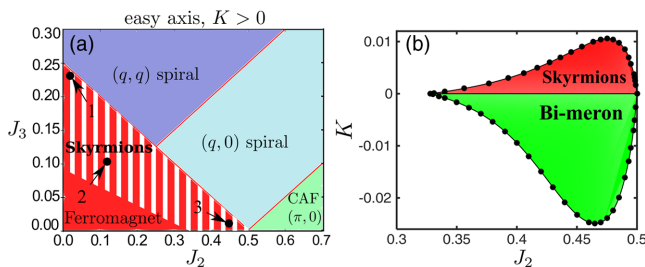stabilize Skyrmions and merons in the FM state.

FIG. 1. (a) $J_2 - J_3$ phase diagram of the square lattice frustrated
magnet with a weak magnetic anisotropy. Stripes show the
stability region of the $Q = 1$ Skyrmion in the FM phase, for
$K = 10^{-3}$. (b) $J_2 - K$ stability diagram of Skyrmions and
bimerons with $Q = 1$, for $J_3 = 0$.

Skyrmions.—The nonlinear sigma model with $\rho > 0$
allows for analytic expression for Skyrmions with an
arbitrary Q found by Belavin and Polyakov [39]. In the
conformally invariant sigma model Skyrmions have no
internal length scale: the energy E_Q of the Skyrmion with
topological charge Q is $4\pi\rho|Q|$ independent of the
Skyrmion size.

The radius R of the Skyrmion with $Q = \pm 1$ (the
elementary Skyrmion) in frustrated magnets is determined
by the competition between the fourth-order terms favoring
infinite R and the easy-axis anisotropy that tends to shrink
the Skyrmion. The dimensional analysis shows that
$R \sim [(b/K)]^{1/4}$, where b is a linear combination of b_1
and b_2 [40]. Skyrmion stability requires $\rho > 0$ and $b > 0$.
In particular, Skyrmions in the Heisenberg model with the
nearest-neighbor interactions only are unstable. Figure 1(b)
shows the stability region of the elementary Skyrmion in
the $J_2 - K$ plane calculated numerically for $J_3 = 0$ [40].
Note that Skyrmions are stable quite far from the
LP $J_2 = 1/2$.

The Skyrmion shape is controlled by the parameters b_1
and b_2, as shown in Figs. 2(a)–(c), and the corresponding
contour plots of the topological charge density $\rho_Q(x,y) =
(1/4\pi)\mathbf{S} \cdot [\partial_x \mathbf{S} \times \partial_y \mathbf{S}]$ [Figs. 2(d)–(f)]. The square-shaped
Skyrmions are observed close to the LPs $(J_2, J_3) =
(1/2, 0)$ and $(J_2, J_3) = (0, 1/4)$. For $J_2 > 2J_3$, the FM
phase transforms into the spiral state with the wave vector $\mathbf{q}$
parallel to the square lattice axes, in which case the
Skyrmion has the shape shown in Figs. 2(a) and 2(d).
For $J_2 < 2J_3$, $\mathbf{q}$ is along the diagonals of squares and the
Skyrmion has the shape shown in Figs. 2(c) and 2(f).

An important difference between Skyrmions for positive
and negative spin stiffness is the form of the Skyrmion-
Skyrmion interaction potential $U_{12}(r)$. For $\rho < 0$, the
potential oscillates, which leads to repulsion or attraction
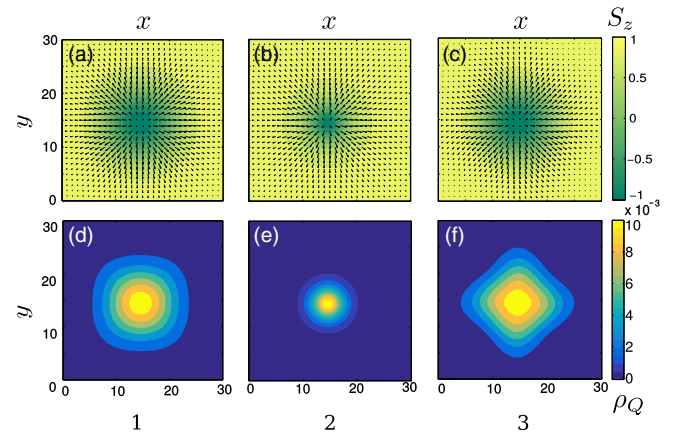depending on the distance r between Skyrmions [33,34].

FIG. 2. (a)–(c) Elementary Skyrmion at the points 1,2,3 on the
phase diagram Fig. 1(a). Arrows show in-plane spin components,
color indicates S_z. (d)–(f) The corresponding contour plots of the
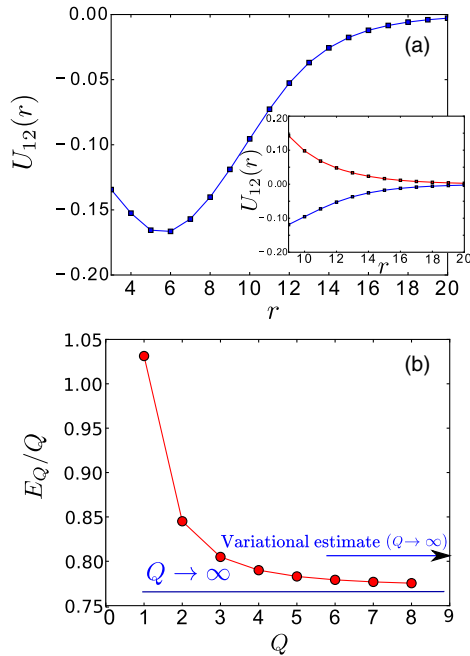topological density, $\rho_Q(x,y)$.

FIG. 3.   (a) Potential energy $U_{12}(r)$ of interaction between two Skyrmions as a function of distance between the centers of the Skyrmions for equal helicities $\chi_1 = \chi_2$ (blue line) and for opposite helicities $\chi_1 - \chi_2 = \pi$ (red line). (b) Energy per Skyrmion E_Q/Q in the Skyrmion ring. The calculations were preformed for $J_2 = 0.2$, $J_3 = 0.149$, and $K = 0.01$.
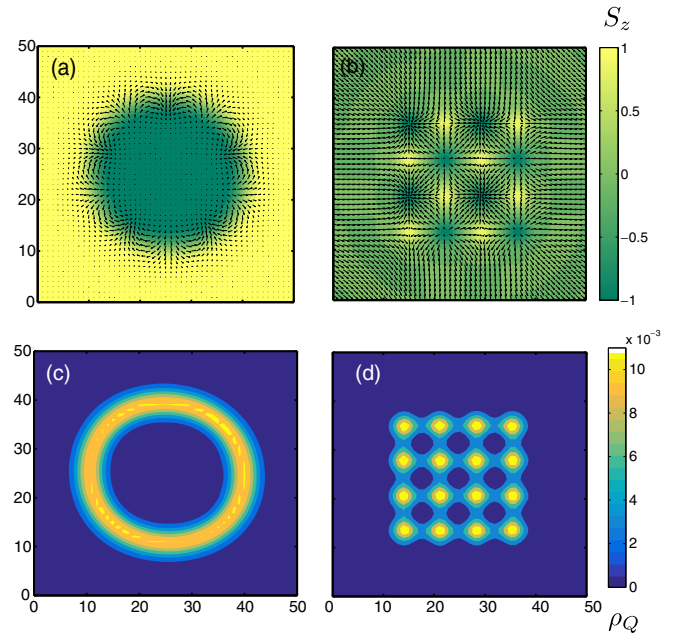

FIG. 4.   (a) The spin configuration of the Skyrmion ring with $Q = -6$ in the frustrated magnet with an easy-axis anisotropy $K = 0.01$ and (c) the corresponding topological charge density distribution $\rho_Q(x, y)$. (b) A meron cluster with a square lattice of vortices and antivortices minimizing energy for topological charge $Q = -8$ and the easy-plane anisotropy $K = -0.01$; (d) the corresponsing $\rho_Q(x, y)$. Other parameters of these simulations are $J_2 = 0.2$ and $\rho = 3 \times 10^{-3}$.

Similar considerations show that for $\rho > 0$, $U_{12}(r)$ remains positive and decreases monotonically at large r. This is also the case for Skyrmions in chiral magnets which repel each other [31,41] because they all have the same helicity angle describing the direction of the in-plane spin components [7]. In easy-axis magnets with competing interactions, the Skyrmion helicity is arbitrary and the repulsion for equal helicities changes to attraction for opposite helicities [see Fig. 3(a)].

Because of the attraction, a multi-Q Skyrmion has a lower energy than Q elementary Skyrmions and can be considered as their bound state. The fact that $U_{12}(r)$ has minimum at $r = r_0$ [see Fig. 3(a)] suggests that the Skyrmion with a large Q occupies the area $\sim Q\pi r_0^2$, so that the Skyrmion radius $R \sim r_0 Q^{1/2}$. Surprisingly, this is not the case: the topological charge and energy densities of the multi-Q Skyrmion are concentrated in a ring of radius $R \sim r_0 Q$ [see Figs. 4(a) and 4(c)].

Figure 3(b) shows that the energy per Skyrmion E_Q/Q decreases with increasing Q and approaches a constant, because the width of the ring and the length of the ring segment occupied by one Skyrmion become Q independent. The energy of Skyrmion in the ring is significantly lower than that of the elementary Skyrmion. This "mass defect" drives the fusion of Skyrmions, which increases the magnitude of the Skyrmion magnetic moment $M_z = \sum_i (S_i^z - 1) < 0$ counted from the positive magnetic

moment of the FM state: for Q elementary Skyrmions $M_z \propto -Q$, whereas for the ring with topological charge Q, $M_z \propto -Q^2$. A magnetic field applied in the positive z direction would lead to fission of multi-Q Skyrmions into Skyrmions with smaller topological charges; see Supplemental Material.

For $Q \gg 1$, we can neglect the ring curvature and consider a straight domain wall with the spiral spin structure, $\mathbf{S} = (\sin\theta(x)\cos qy, \sin\theta(x)\sin qy, \cos\theta(x))$, separating the $S_z = -1$ FM state at $x < 0$ from the $S_z = +1$ FM state at $x > 0$. The length of the wall in the y direction is $L_y = 2\pi R = (2\pi Q/q)$. Using a variational ansatz for the wall shape $\cos\theta(x) = -\tanh(\varkappa x)$, where $\varkappa$ is the inverse domain wall width, we obtain

$$\frac{E_Q}{Q} = \frac{2\pi}{q\varkappa}\left(\rho(q^2 + \varkappa^2) + b_1(q^4 + \varkappa^4) + \frac{b_2}{3}q^2\varkappa^2 + K\right). \quad (3)$$

Minimization with respect to q and $\varkappa$ gives $\varkappa = |q| = \{K/[2b_1 + (1/3)b_2]\}^{1/4}$ and

$$\frac{E_Q}{|Q|} = 4\pi\left(\rho + \sqrt{K\left(2b_1 + \frac{1}{3}b_2\right)}\right). \quad (4)$$

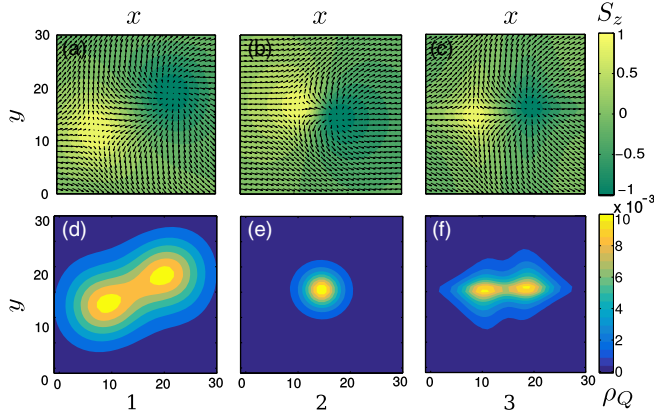Note that the first term in Eq. (4) is the lower bound for the energy of the multi-Q Skyrmion in the nonlinear sigma

FIG. 5. (a)–(c) Deconfinement of meron pairs in a frustrated magnet with an easy-plane anisotropy $K < 0$ for J_2 and J_3 at the points (1,2,3) on the phase diagram in Fig. 1(a). (d)–(f) Topological density ρ_Q for the spin configurations in (a)–(c). In panels (a),(d) and (c),(f) the system is close to the FM-spiral phase boundary, which results in the topological "fractionalization," i.e., a spatial separation of merons.

model [39] and that $\varkappa$, q and $E_Q/|Q|$ are indeed independent of Q. The domain wall stability requires $6b_1 + b_2 > 0$ (or $4J_2 + 16J_3 > J_1$) and this result can be shown to be independent of the orientation of the wall with respect to the crystal axes. The binding energy makes multi-Q Skyrmions more stable than elementary Skyrmions [40].

Merons.—So far we discussed magnets with an easy-axis anisotropy. For an easy-plane anisotropy ($K < 0$), the topological defect with $Q = 1$ is a bound state of vortex and antivortex (see Fig. 5). The sign of the out-of-plane magnetization in the core of the vortex is opposite to that in the antivortex core, so that each half of the Skyrmion, called meron, has $Q = \frac{1}{2}$.

The emergence of vortices and antivortices is related to the spontaneous breaking of $O(2)$ rotational symmetry by the uniform in-plane magnetization. The bimeron configuration in the FM state with $S_x = +1$ can, to a good approximation, be obtained from the Skyrmion configuration for the $S_z = +1$ state by $\pi/2$ rotation around the y axis: $(S_x, S_y, S_z) \to (S_z, S_y, -S_x)$, which explains the similarity between the stability diagrams for Skyrmions and meron pairs in the $J_2 - J_3$ and $J_2 - K$ planes [Figs. 1(a) and 1(b) and Fig. 2 of the Supplemental Material].

Near a LP the distance between merons is large giving rise to two distinct peaks in the distribution of topological charge density [Figs. 5 (a), 5(d), 5(c), and 5(f)]. The fractionalization of Skyrmion occurs because the two-dimensional Coulomb potential that confines vortex to an antivortex [42],

$$U_C(r) = 2\pi\rho \ln(r/r_0), \qquad (5)$$

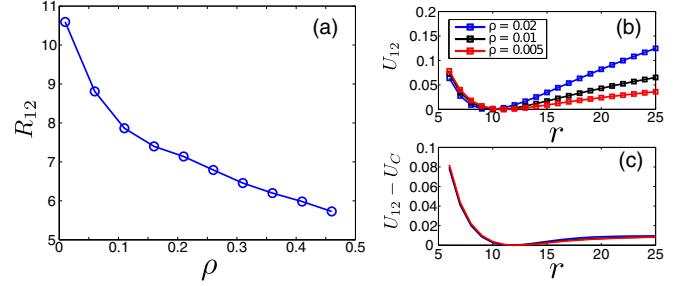r_0 being the meron radius, vanishes at the LP $\rho = 0$.

FIG. 6. (a) Optimal distance between the centers of merons R_{12} vs spin stiffness. R_{12} increases near the LP $\rho = 0$ resulting in a fractionalization of topological charge. (b) The meron-meron interaction potential U_{12} vs the distance between merons. (c) The "non-Coulomb" part of the interaction potential $U_{12} - U_C$ vs meron-meron distance. The model parameters are $K = -5 \times 10^{-3}$ and $J_3 = 0.1$. The minimum of the potential energy curves is shifted to zero.

Figure 6(a) shows that at zero temperature the deconfinement of merons is incomplete: at the LP the optimal distance between merons R_{12} remains finite, because the meron-meron interaction energy $U_{12}(r)$ has a minimum even at $\rho = 0$ [Figs. 6(b) and 6(c)]. The bimeron molecules will, however, dissociate at $T \neq 0$. Metastable Skyrmions and their bound states exist also at nonzero temperatures and are subjected to Brownian motion [43].

At large distances bimerons interact via two-dimensional dipole-dipole interactions [45] resulting in formation of multimeron bound states. For $Q \gg 1$, the minimal-energy configuration is the square lattice formed by merons [Figs. 4(c) and 4(d)], analogous to the simple cubic lattice of half-Skyrmions in nuclear physics [6].

Discussion and conclusions.—We showed that metastable Skyrmions and merons can exist in two-dimensional ferromagnets with conventional centrosymmetric lattices. Magnetic frustration required for stabilization of these topological excitations is considerably weaker than the one that destabilizes the FM state. Skyrmions in easy-axis magnets attract each other and in absence of magnetic field form long lines or rings facilitating their observation by Lorentz transmission electron microscopy [46] and spin-polarized scanning tunnelling microscopy [47]. Skyrmions can be created by injecting a vertical spin-polarized electric current perpendicular to the plane of a frustrated magnet film or alternatively by using thermal annealing (Kibble-Zureck mechanism [48]) or local heating [49]. The collapse of multi-Skyrmion bound states in an applied magnetic field can be observed in measurements of the discretized Hall resistivity in nanostructured Hall bars [50].

Skyrmion bound states with $Q \gg 1$ resemble hard bubbles in thin ferromagnetic films with $2(Q - 1)$ Bloch lines [51]. However, hard bubbles do not form because of attraction between the elementary bubbles and, in general, they do not minimize energy for a given value of topological charge.

PHYSICAL REVIEW LETTERS

They are also much bigger in size and require both applied magnetic field and strong perpendicular anisotropy.

Bound states of magnetic Skyrmions bare similarity to Skyrmions with large baryonic numbers modeling nuclei. In the chiral limit of vanishing pion mass the minimal energy solutions of the Skyrme model are hollow polyhedra with the baryon density concentrated in a relatively thin nuclear sphere [3], resembling the topological rings [Figs. 4(a) and 4(c)]. The nonzero pion mass leads to a collapse of the nuclear sphere, similar to the collapse of the multi-Q Skyrmions in a magnetic field. The magnetization patterns in the topological ring and bimeron resemble the distribution of orbital momentum of Cooper pairs in topological defects in the A phase of superfluid helium-3 (cf. Fig. 1 in [52]).

Our results are directly relevant for square-lattice ferromagnets [53], and, qualitatively, they hold for other lattice types including layered antiferromagnets with a weak AFM coupling between FM layers. In particular, bimerons can exist in the collinear phase of the easy-plane triangular antiferromagnet NiBr$_2$ [54]. Pressure and chemical substitutions can be used to tune frustrated magnets across the Lifshitz point.

---

[1] T. H. R. Skyrme, Nucl. Phys. **31**, 556 (1962).
[2] I. Zahed and G. E. Brown, Phys. Rep. **142**, 1 (1986).
[3] R. A. Battye, N. S. Manton, and P. M. Sutcliffe, in *The Multifaceted Skyrmions* (World Scientific, Singapore, 2016).
[4] I. R. Klebanov, Nucl. Phys. **B262**, 133 (1985).
[5] A. S. Goldhaber and N. S. Manton, Phys. Lett. B **198**, 231 (1987).
[6] M. Kugler and S. Shtrikman, Phys. Rev. D **40**, 3421 (1989).
[7] N. Nagaosa and Y. Tokura, Nat. Nanotechnol. **8**, 899 (2013).
[8] S. L. Sondhi, A. Karlhede, S. A. Kivelson, and E. H. Rezayi, Phys. Rev. B **47**, 16419 (1993).
[9] S. E. Barrett, G. Dabbagh, L. N. Pfeiffer, K. W. West, and R. Tycko, Phys. Rev. Lett. **74**, 5112 (1995).
[10] T. Ho, Phys. Rev. Lett. **81**, 742 (1998).
[11] G. E. Volovik, *The Universe in a Helium Droplet* (Clarendon Press, Oxford, England, 2003).
[12] J. Fukuda and S. Zumer, Nat. Commun. **2**, 246 (2011).
[13] A. N. Bogdanov and D. A. Yablonskii, Sov. Phys. JETP **68**, 101 (1989).
[14] S. Mühlbauer, Science **323**, 915 (2009).
[15] X. Z. Yu, Y. Onose, N. Kanazawa, J. H. Park, J. H. Han, Y. Matsui, N. Nagaosa, and Y. Tokura, Nature (London) **465**, 901 (2010).
[16] F. Jonietz *et al.*, Science **330**, 1648 (2010).
[17] X. Z. Yu, N. Kanazawa, W. Z. Zhang, T. Nagai, T. Hara, K. Kimoto, Y. Matsui, Y. Onose, and Y. Tokura, Nat. Commun. **3**, 988 (2012).
[18] J. S. White *et al.*, Phys. Rev. Lett. **113**, 107203 (2014).
[19] S. Seki, X.Z Yu, S. Ishiwata, and Y. Tokura, Science **330**, 1648 (2012).
[20] M. Mochizuki, X. Z. Yu, S. Seki, N. Kanazawa, W. Koshibae, J. Zang, M. Mostovoy, Y. Tokura, and N. Nagaosa, Nat. Mater. **13**, 241 (2014).
[21] A. Fert, V. Cros, and J. Sampaio, Nat. Nanotechnol. **8**, 152 (2013).
[22] J. Iwasaki, M. Mochizuki, and N. Nagaosa, Nat. Nano-technol. **8**, 742 (2013).
[23] Y. Zhou and M. Ezawa, Nat. Nanotechnol. **5**, 4652 (2014).
[24] W. Jiang *et al.*, Science **349**, 283 (2015).
[25] C. Moreau-Luchaire *et al.* Nat. Nanotechnol. **11**, 444 (2016).
[26] S. Woo *et al.*, Nat. Mater. **15**, 501 (2016).
[27] L. Brey, H. A. Fertig, R. Cote, and A. H. MacDonald, Phys. Scr. T **T66**, 154 (1996).
[28] R. Cote, W. Luo, B. Petrov, Y. Barlas, and A. H. MacDonald, Phys. Rev. B **82**, 245307 (2010).
[29] M. Ezawa, Phys. Rev. B **83**, 100408(R) (2011).
[30] S. Z. Lin, A. Saxena, and C. D. Batista, Phys. Rev. B **91**, 224407 (2015).
[31] U. K. Rößler, A. A. Leonov, and A. N. Bogdanov, J. Phys. Conf. Ser. **303**, 012105 (2011).
[32] T. Okubo, S. Chung, and H. Kawamura, Phys. Rev. Lett. **108**, 017206 (2012).
[33] A. O. Leonov and M. Mostovoy, Nat. Commun. **6**, 8275 (2015).
[34] S. Z. Lin and S. Hayami, Phys. Rev. B **93**, 064430 (2016).
[35] L. Balents and O. A. Starykh, Phys. Rev. Lett. **116**, 177201 (2016).
[36] A. Milstein and O. P. Sushkov, Phys. Rev. B **84**, 195138 (2011).
[37] L. Seabra, P. Sindzingre, T. Momoi, and N. Shannon, Phys. Rev. B **93**, 085132 (2016).
[38] See the Supplemental Material at http://link.aps.org/supplemental/10.1103/PhysRevLett.119.207201 for discussion. This holds for isotropic Heisenberg model. $K > 0$ extends the region of stability of the FM state.
[39] A. A. Belavin and A. M. Polyakov, JETP Lett. **22**, 245 (1975).
[40] See the Supplemental Material at http://link.aps.org/supplemental/10.1103/PhysRevLett.119.207201 for details of variational and numerical calculations and the discussion of stability of multi-Q Skyrmions.
[41] Small Skyrmions in thin films can attract each other; see L. Rózsa, A. Deák, E. Simon, R. Yanes, Lá. Udvardi, L. Szunyogh, and U. Nowak, Phys. Rev. Lett. **117**, 157205 (2016).
[42] J. M. Kosterlitz and D. J. Thouless, J. Phys. C **6**, 1181 (1973).
[43] See the Supplemental Material at http://link.aps.org/supplemental/10.1103/PhysRevLett.119.207201 where we present movies showing Brownian motion of Skyrmions. Finite temperature dynamics of Skyrmions was simulated using the approach described in Ref. [44].
[44] S.-Z. Lin, C. D. Batista, C. Reichhardt, and A. Saxena, Phys. Rev. Lett. **112**, 187203 (2014).
[45] D. Gross, Nucl. Phys. **B132**, 439 (1978).
[46] T. Tanigaki, K. Shibata, N. Kanazawa, X. Yu, Y. Onose, H. S. Park, D. Shindo, and Y. Tokura, Nano Lett. **15**, 5438 (2015).

[47] N. Romming, C. Hanneken, M. Menzel, J. E. Bickel, B. Wolter, K. von Bergmann, A. Kubetzka, and R. Wiesendanger, Science **341**, 636 (2013).

[48] T. W. B. Kibble, J. Phys. A **9**, 1387 (1976); W. H. Zurek, Nature (London) **317**, 505 (1985).

[49] W. Koshibae and N. Nagaosa, Nat. Commun. **5**, 5148 (2014).

[50] N. Kanazawa, M. Kubota, A. Tsukazaki, Y. Kozuka, K. S. Takahashi, M. Kawasaki, M. Ichikawa, F. Kagawa, and Y. Tokura, Phys. Rev. B **91**, 041122 (2015).

[51] A. P. Malozemoff and J. C. Slonczewski, *Magnetic Domain Walls in Bubble Materials* (Academic Press, New York, 1979).

[52] Ü. Parts, J. M. Karimäki, J. H. Koivuniemi, M. Krusius, V. M. H. Ruutu, E. V. Thuneberg, and G. E. Volovik, Phys. Rev. Lett. **75**, 3320 (1995).

[53] N. Shannon, B. Schmidt, K. Penc, and P. Thalmeier, Eur. Phys. J. B **38**, 599 (2004).

[54] P. Day, A. Dinsdale, E. R. Krausz, and D. J. Robbins, J. Phys. C **9**, 2481 (1976).